Data-Driven Additive Manufacturing Constraints for Topology Optimization

Benjamin M Weiss
University of Washington
Seattle, WA, USA

Joshua M Hamel
Seattle University
Seattle, WA, USA

Mark A Ganter
University of Washington
Seattle, WA, USA

Duane W Storti
University of Washington
Seattle, WA, USA

ABSTRACT

The topology optimization (TO) of structures to be produced using additive manufacturing (AM) is explored using a data-driven constraint function that predicts the minimum producible size of small features in different shapes and orientations. This shape- and orientation-dependent manufacturing constraint, derived from experimental data, is implemented within a TO framework using a modified version of the Moving Morphable Components (MMC) approach. Because the analytic constraint function is fully differentiable, gradient-based optimization can be used. The MMC approach is extended in this work to include a "bootstrapping" step, which provides initial component layouts to the MMC algorithm based on intermediate Solid Isotropic Material with Penalization (SIMP) topology optimization results. This "bootstrapping" approach improves convergence compared to reference MMC implementations. Results from two compliance design optimization example problems demonstrate the successful integration of the manufacturability constraint in the MMC approach, and the optimal designs produced show minor changes in topology and shape compared to designs produced using fixed-radius filters in the traditional SIMP approach. The use of this data-driven manufacturability constraint makes it possible to take better advantage of the achievable complexity in additive manufacturing processes, while resulting in typical penalties to the design objective function of around only 2% when compared to the unconstrained case.

NOMENCLATURE

$\mathbf{c}^k$	Parameters for the kth morphable component
$E; E_{min}$	Elastic modulus of fully dense; void material
$\mathbf{F}$	Applied load
f	Objective function (compliance)
$\bar{f}$	Thresholded compliance
H	Smoothed Heaviside function
$\mathbf{K}$; $\mathbf{k}_e$	Global stiffness matrix; stiffness matrix for element e
$\mathbf{k}_0$	Stiffness matrix for a fully-dense element
l	Feature/component length

l_{min}	Minimum allowed initial component length
p	Density penalization exponent
$S(l,\theta)$	Data-driven continuous constraint function
$t; t^k$	Thickness; thickness of component k
t_{min}^k	Minimum allowable thickness for component k
Δt^k	Manufacturability margin for component k
$\mathbf{U};\ \mathbf{u}_e$	Displacement; displacement for element e
V_f	Allowable volume fraction of solid material
$\mathbf{z}$	Optimization decision variable (exact usage varies)
γ	Smoothing for bulk density Heaviside function
ϵ	Smoothing for edge transition Heaviside function
ϕ	Distance field from morphable components
$\bar{\rho}; \bar{\rho}^k$	Bulk density; bulk density of component k
ρ_e	Density of finite element e
θ	Feature/component angle from build direction

INTRODUCTION

Additive manufacturing (AM) has become a compelling alternative to traditional manufacturing technologies for the fabrication of complex, organic shapes produced by topology optimization [1]. The ability of AM to inexpensively produce complex shapes has led to a variety of topology optimization applications including mesostructured or lattice materials [2][3]. However, despite the advantages AM provides over traditional manufacturing processes in the context of the fabrication of topology optimized designs, AM also brings with it unique manufacturing challenges [4].

Liu and Ma [1] provide a summary of recent work in this area, and by and large researchers have focused on applying two kinds of manufacturing constraints from the AM process within topology optimization problems: the *minimum feature size* (or the smallest element of a design which can be realized by the manufacturing process), and the *overhang angle* (the maximum degree of overhang achievable by the process without requiring support structures). Efforts involving feature size and overhang angle constraints are valuable but must necessarily ignore much of the complex interactions between feature shape, orientation, and manufacturability, and thus typically lead to overly conservative designs in an effort to ensure manufacturability. AM processes are capable of producing some features not permitted by these constraints, and constraints which more accurately reflect the real process capabilities should make more performant designs possible. For many optimization objectives, theoretical work indicates that the optimal designs consist of infinitely many infinitely small members, so the ability to produce smaller members

increases the optimality of the design [5]. Clearly, better strategies for including the true and complex capabilities of AM systems into topology optimization frameworks are needed to take full advantage of the benefits of TO, and this this work seeks to address that need.

In previous work, the authors developed a new design constraint for AM processes by experimentally determining minimum feature size as a continuous function of feature shape and build orientation [6][7][8]. The resulting function can be used to account for both overhang and minimum feature size effects simultaneously by applying a penalty to unsuitable features, thus capturing more closely the true capabilities of an AM process to produce a desired geometry. Note that these design rules do not consider the mechanical capability or surface finish of a resulting part. This work presents an effort to use this previously developed parametric constraint function within a topology optimization algorithm, presenting a new way of formulating the minimum feature size constraint based on the shape and orientation of each design feature. To accomplish this, the Moving Morphable Component (MMC) framework [9] is adapted to obey the functional feature size constraint and "bootstrapped" (i.e. provided with initial conditions) using the Solid Isotropic Material with Penalization (SIMP) method [10]. The new method is termed the "bootstrapped constrained Moving Morphable Components", or bcMMC approach.

The rest of this paper is laid out as follows. First a brief literature review is provided that presents the necessary background information for understanding the bcMMC approach and how this new approach differs from existing techniques. Then the details of the manufacturing constraint and the bootstrapping process used are presented. Finally, the bcMMC approach is applied to multiple topology optimization test problems, and the obtained results are presented and discussed.

BACKGROUND

The topology optimization problem seeks to divide a design domain into solid ($\rho = 1$) and void ($\rho = 0$) regions in order to minimize an objective function; the objective considered here is compliance minimization. Two recent surveys cover the vast literature in this field [11][12], and only a brief introduction to two solution approaches is given here.

In this work, the domain is divided into uniform rectangular finite elements. The general problem statement is given by:

$$\min_{\mathbf{z}}: \quad f(\mathbf{z},\mathbf{U}) = \sum_{e=1}^{n_e} \mathbf{u}_e^T \mathbf{k}_e(\rho_e(\mathbf{z}))\mathbf{u}_e \tag{1a}$$

$$\mathbf{k}_e(\rho_e(\mathbf{z})) = \left[E_{min} + \rho_e^p(\mathbf{z})(E - E_{min})\right]\mathbf{k}_0 \tag{1b}$$

$$\text{subject to}: \quad \mathbf{KU} = \mathbf{F} \tag{1c}$$

$$\frac{1}{n_e}\sum_{e=1}^{n_e} \rho_e(\mathbf{z}) - V_f \leq 0 \tag{1d}$$

$$\mathbf{z}_{min} \leq \mathbf{z} \leq \mathbf{z}_{max} \tag{1e}$$

where the state variable $\mathbf{U}$ is the element displacements, each of the n_e elements having a stiffness $\mathbf{k}_e$ set by its individual density ρ_e which is controlled by the decision variable $\mathbf{z}$, which is varied by the optimizer and governs the distribution of material within the domain. The linear elastic relationship is the state equation, where $\mathbf{F}$ is the vector of applied loads and $\mathbf{K}$ the global stiffness matrix. The volume constraint V_f restricts the total fraction of solid elements.

In the SIMP approach, the decision variable $\mathbf{z}$ represents the continuous density of each element, i.e. $\rho_e(\mathbf{z}) = z_e$ and $\mathbf{z}_{min} = \mathbf{0}; \mathbf{z}_{max} = \mathbf{1}$. Solid/void solutions are encouraged by penalizing the elastic modulus of intermediate-density elements using Eqn. (1b) where E and E_{min} are the elastic modulus of solid and void elements, respectively; $\mathbf{k}_0$ is the fully dense element stiffness matrix; and p is a penalization constant set to 3.0 [9]. The optimized structure is developed implicitly as the decision variable sets the density of each element; post-processing converts this grayscale image to a smooth manufacturable design. To ensure the created structures are accurately modelled by within a finite element analysis (FEA) study, the filtering approach of Guest et al. [13] is employed to enforce a constant minimum thickness of all solid regions.

Moving Morphable Components

In contrast to the implicit SIMP approach, the MMC framework defines geometry explicitly, using the decision variable $\mathbf{z}$ to instead define control points on a set of parametric primitive shapes ("morphable components") which are projected onto the design domain to set element densities [14]. The new approach described later in this paper is an adaptation of the MMC formulation described below, which is itself adapted from Refs. [14][15][16].

The design domain is pre-populated with components each consisting of the offset of a line segment parameterized by endpoint locations and offset distance (thickness); see Figure 1. The decision variable is constructed by combining the parameters of each component, i.e. $\mathbf{z} = \left[(\mathbf{c}^1)^{\mathrm{T}}, (\mathbf{c}^2)^{\mathrm{T}}, \dots, (\mathbf{c}^k)^{\mathrm{T}}, \dots, (\mathbf{c}^{n_c})^{\mathrm{T}}\right]^{\mathrm{T}}$, with the parameter of the kth component $\mathbf{c}^k = \left[x_1^k, y_1^k, x_2^k, y_2^k, t^k\right]^{\mathrm{T}}$. Let $\phi(x, y, \mathbf{c}^k)$ be the signed Euclidian distance (interior positive) from a point (x, y) on the domain to the component defined by $\mathbf{c}^k$, following the approach of Eqn. 4 in Deng and Chen [14].

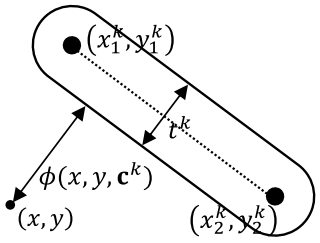

Figure 1. Schematic of Component $\boldsymbol{k}$

To construct the density field, a smoothed Heaviside function is applied to the distance field for each component at each finite element centroid, according to:

$$H(\phi,\epsilon,\bar{\rho}) = \begin{cases} \bar{\rho} & \text{if } \phi > \epsilon \\ \frac{3\bar{\rho}}{4}\left(\frac{\phi}{\epsilon} - \frac{\phi^3}{3\epsilon}\right) + \frac{\bar{\rho}}{2} & \text{if } -\epsilon \le \phi \le \epsilon \\ 0 & \text{otherwise} \end{cases} \tag{2}$$

with parameters ϕ, the distance to the component (arguments to ϕ omitted for clarity); ϵ the regularization parameter describing the width of the transition; and $\bar{\rho}$, the bulk density of the component (i.e. 1.0). In this way elements smoothly transition from void (outside) to $\bar{\rho}$ (inside) over a band of size 2ϵ. The density of FEA element e (denoted ρ_e) is assigned by sampling this function at the element centroid (x_e, y_e) for each component and retaining the maximum:

$$\rho_e(\mathbf{z}) = \max_{k=1..n_c} H\left(\phi\left(x_e, y_e, \mathbf{c}^k\right), \epsilon, \bar{\rho}\right). \\ \text{Note that } \mathbf{z} = [(\mathbf{c}^1)^{\mathrm{T}}, (\mathbf{c}^2)^{\mathrm{T}}, \ldots, (\mathbf{c}^{n_c})^{\mathrm{T}}]^{\mathrm{T}},\ \bar{\rho} = 1 \tag{3}$$

Unlike SIMP, the design variable $\mathbf{z}$ consists of the parameters of all the components; as a result, the minimum and maximum bounds on $\mathbf{z}$ are more complex, dependent on the domain shape and range of acceptable element thicknesses.

Derivatives are computed using the chain rule. Equations (1a) and (1b) provide the derivative of f with respect to element density ρ_e; the derivative with respect to the decision variables $\mathbf{z}$ can be obtained as

$$\frac{\partial f}{\partial z_j} = \sum_{e=1}^{n_e} \frac{\partial f}{\partial \rho_e}\frac{\partial \rho_e}{\partial z_j} \\ \frac{\partial f}{\partial \rho_e} = -p\rho_e^{p-1}(1 - E_{min})\mathbf{u}_e^T\mathbf{k}_0\mathbf{u}_e \tag{4}$$

For implementation convenience, the derivative of each density with respect to each design variable is computed numerically, following the approach of Refs. [14][16]. This derivative could be constructed explicitly by replacing the *max* function in Eqn. (3) with a "*softmax*" alternative. In this work when reporting and comparing objective function values, the "thresholded compliance" will be used, denoted $\bar{f}$ and constructed by thresholding the densities in the design domain so as to satisfy the volume constraint.

Bootstrapping Approaches

"Bootstrapping" refers to the idea of leveraging existing resources to produce a more complex or capable outcome. Here, bootstrapping refers to using SIMP to select the starting locations for components in the

MMC process, described in detail shortly. Similar concepts have been explored by Bremicker et al. [17], who extracted a topology from a SIMP solution and used it as the starting point for shape optimization, leveraging a computer vision technique to produce a shape skeleton, or single-pixel-wide backbone of a shape [18]. Similar chaining of topology and subsequent shape optimization are used under human direction in engineering practice, for an example see Chang and Tang [19].

In a recent review, Sigmund and Maute [12] point out the need for more topology optimization research in "hybrid approaches" in which the benefits of two topology optimization approaches are combined to remove initial condition sensitivity and improve convergence. While not the primary contribution of this work, the approach presented here also begins to address this need.

Manufacturing Constraints in Topology Optimization

Liu and Ma [1] review various approaches for incorporating manufacturing constraints into the topology optimization problem in order to avoid post-processing steps which often destroy the local optimality of the solution. For AM, two most-studied constraints are the minimum feature size and the maximum overhang angle.

Minimum feature size has long been integrated into the SIMP approach in order to produce mesh-dependent designs (i.e. through filtering the density field), and Lazarov et al. [20] survey these approaches in the context of manufacturability. Recently, an approach which adapts this filter to the direction-dependent feature size characteristic of most AM processes has also been presented [21]. In the MMC framework, minimum feature size for each component can be explicitly constrained, but narrow hinges can still form where two members overlap just slightly, as explored by Hoang and Jang [22].

Overhang angle has also been studied, but far less extensively [23][24][25][26]. Some authors utilize asymmetric filters and projections in a framework similar to SIMP, to ensure that solid elements are only allowed in locations with appropriate support leading to optimized structures containing many small elements which simultaneously bear load and support structures that would otherwise not be manufacturable [23][24][26]. Typically, these approaches incur a penalty to the objective function of 2-10% when applied to standard test problems.

Guo et al. [25] built specific constraints into the formulation of their MMC and Moving Morphable Voids (MMV) approaches to ensure the result follows the overhang angle constraint. This works well in their MMC implementation, in which the orientation of the part on the build plate is included as a decision variable and results in only 1% increase in the objective function compared to an unconstrained design. Their MMV approach does not include orientation as a decision variable and the resulting geometry differs significantly from the optimal, with a corresponding 14% penalty in the objective function. Liu and Ma [1]

cite overhang angle constraints as a significant unsolved problem in topology optimization for AM, noting the substantial change in shape and objective function value seen in most approaches.

DATA-DRIVEN MANUFACTURING CONSTRAINTS

In this section, the conceptual basis for the proposed additive manufacturing constraint is presented. In previous work [7][8], a piecewise-continuous, polynomial minimum feature size design rule function for small features produced by an AM platform was presented. The generated design rule returns the minimum manufacturable diameter of a beam given its length and angle from the build direction as shown in Figure 2.

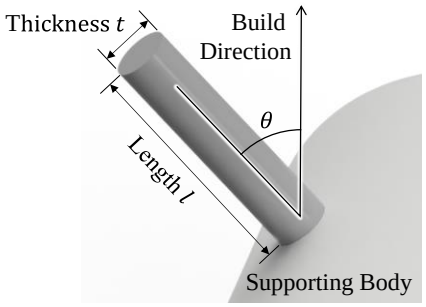

Figure 2. Schematic of a Small Feature

Instead of imposing an explicit overhang constraint, the proposed approach requires all features to be manufacturable as determined by a predetermined design rule function. Because overhanging features in the process studied exhibit surface defects in the downward direction, correspondingly larger minimum feature thicknesses were obtained, suitably penalizing these difficult-to-manufacture features. The experimental data collected also includes horizontal "bridging" features which connect two supporting bodies. This ability to incorporate bridges with experiment-driven sizing information is a significant advantage of the present approach over overhang angle constraints, as it allows some manufacturable horizontal features in the final design.

For the present work, the 2D optimized structure is assumed to extend a relatively small distance into the plane, and manufacturing constraints from small cylinders are assumed valid for the rectangular cross-section of the 2D features extended uniformly into the plane. The experimentally-determined constraint function for a material extrusion machine, including bridging data, are shown in Figure 3 and denoted $S(l, \theta)$ where l is the feature length and θ is the angle between the feature axis and the build direction. Once the size of a feature (e.g. S) is known, this function can be used to determine if a feature will be manufacturable or not based on its orientation (e.g. l and θ). This manufacturability constraint function is assumed to be already known at the start of the optimization process and is not derived in this work. Readers

are directed to [7][8] for information on how to generate a manufacturability function for an AM system of interest.

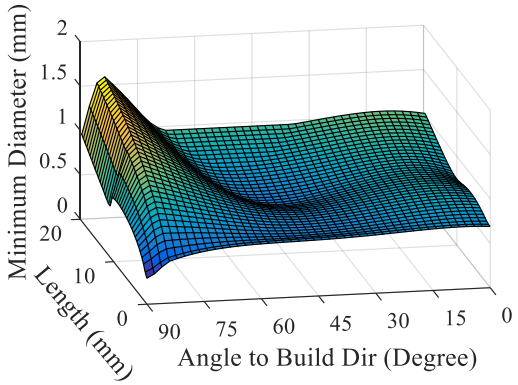

Figure 3. The Parametric Constraint Function

BOOTSTRAPPED CONSTRAINED MOVING MORPHABLE COMPONENTS

In this section, the details of the bcMMC approach are presented, which builds on the MMC method described above. Specific extension to the MMC method are described, including the integration of the data-driven manufacturing constraint and the bootstrapping method used. After a brief overview, subsections present details of the bootstrapping process and the constrained MMC method.

Overview

Figure 4 shows an overview of the bcMMC algorithm, which consists of two phases, an initial bootstrapping phase and a main constrained optimization phase. It takes as input an optimization domain, load and support conditions, and a build direction (Figure 4a). In the bootstrapping phase, a SIMP solution with fixed minimum feature size is computed (Figure 4b). Then, the density field is converted into a set of connected morphable components (Figure 4c) which serve as the starting configuration for the constrained optimization. This is described in the Phase 1 subsection below.

In Phase 2, the MMC optimizer adjusts the component endpoints and thicknesses to minimize the objective (Figure 4d). At each iteration, the minimum manufacturable thickness for each component is assessed using the constraint function described previously (Figure 4e). As the thickness of each component approaches the minimum manufacturable value, its bulk density is smoothly reduced from fully dense to void. Each component is projected to the new density field (Figure 4f), FEA and sensitivity calculations are performed, and the optimizer updates the decision variables (Figure 4g). The process repeats until a convergence criterion is reached as described in the “Phase 2” subsection below.

For example, consider the component labelled with a triangle in Figure 4d. On each iteration, the component’s orientation, length, and thickness are used to place it in the manufacturability space, which

assigns it a "manufacturability margin" based on the difference between the current thickness (triangle in Figure 4e) and the constraint surface. In this case, the triangle is near the constraint surface and marginally manufacturable, so it is assigned an intermediate bulk density, which is used when the component is projected onto the FEA element grid (Figure 4f).

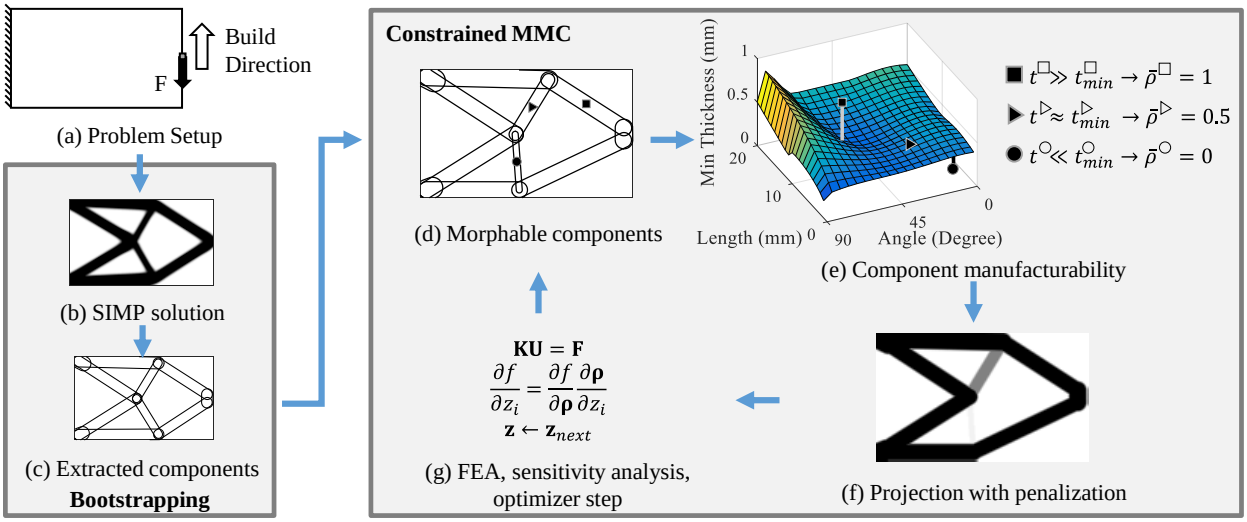

Figure 4. Flowchart of the bcMMC Process (see text for description)

Phase 1: Bootstrapping

In this subsection, the bootstrapping approach which provides the main optimizer with an intelligent and connected initial component configuration is detailed. The SIMP algorithm is used to provide a preliminary component layout for the constrained optimization procedure described in the next subsection, producing a "bootstrapped constrained" MMC or bcMMC approach. Bootstrapping provides a dramatic improvement in convergence to a stable equilibrium(measured in both compute time and iteration count) compared with an MMC solution initialized with arbitrarily-distributed components. However, the search space is narrowed by starting the MMC optimization near a local minimum without the opportunity to explore different and possibly more performant areas of the search space. Note that the main algorithm can still effect topology changes by overlapping or penalizing members which it deems inefficient in light of the manufacturing constraints. This procedure follows in the spirit of Bremicker et al. [17], who used the shape skeleton as a means to extract features from a SIMP solution.

Here, the SIMP algorithm is first run for a small number of iterations to produce an initial solution to the optimization problem under a fixed minimum feature size that is just less than the smallest manufacturable feature (see Figure 5a). SIMP quickly converges from a uniform initial condition (i.e. gray; not shown) to the vicinity of a local optimum, reducing the need for the MMC algorithm to slowly move components over long distances.

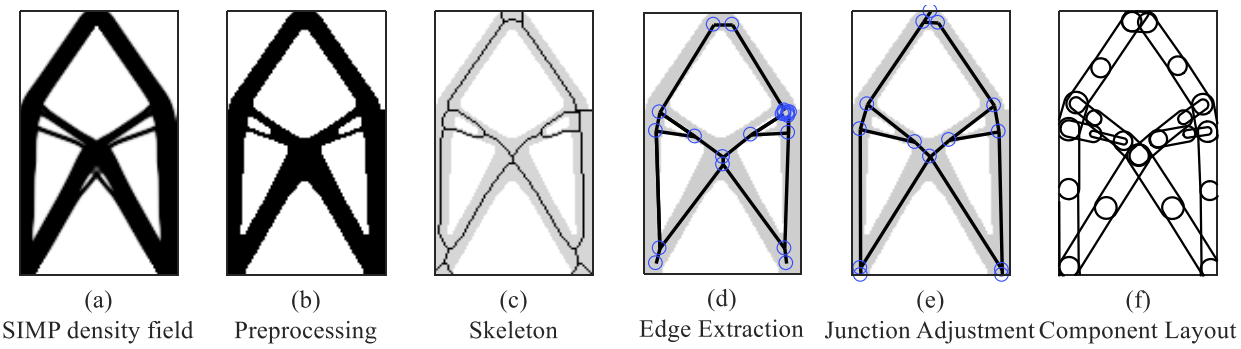

Figure 5. Bootstrapping Procedure (see text for details)

To create the initial component layout, the SIMP density field is first preprocessed by applying a threshold to the grayscale design and using a morphological closing operation to eliminate small holes (Figure 5b). The shape skeleton is then computed (Figure 5c). By design, the shape skeleton preserves the topology of the input, but converts all members to single-pixel-wide features. The junction points in the skeleton, where two or more skeletal branches come together, are extracted.

Adjacent junction points in the skeletal graph are connected with straight segments (Figure 5d). Each segment will form the center line of a component. Segments which are shorter than a pre-determined threshold, l_{min}, are removed and nearby junction points merged. In order for each linear component to more precisely reflect the original shape, the locations of all junction points are moved so as to minimize the deviation of the linear segments from the center lines of the features in the density field (Figure 5e). In addition, new component segments are added to connect the skeleton to each of the load or support points in the problem setup, ensuring that the design does not become disconnected from the boundaries.

To provide the optimizer with additional flexibility in determining the shape and structure of the final design, long components (in this case those with length greater than $5l_{min}$) are divided in half, with a new junction point inserted at the midpoint and initial thicknesses set according to the average thickness of the corresponding region of the SIMP design, scaled so as to respect the volume constraint (Figure 5f).

Phase 2: Constrained MMC Optimization

Two key modifications of the MMC framework are presented to enforce the manufacturing constraint: (1) the components are explicitly and inexorably connected, and (2) the density of unmanufacturable features is penalized.

For reasons described later, it is desirable to explicitly link the end points of each component to its neighbors. The bootstrapping process provides this linkage information, and the structure of the decision variable $\mathbf{z}$ is changed from that presented in the Background to consist of a series of junction point coordinates followed by a series of component thicknesses, while the mapping between junction points and

thicknesses is tracked separately. This is similar to the Connected Morphable Components of Ref. [14]; however, in the present work more than two components can share a junction.

At each update in the new bcMMC framework, the kth component is assigned a minimum thickness value, $t_{min}^k = t_{min}(\mathbf{c}^k) = S(l^k, \theta^k)$ based on its length l^k and orientation θ^k, which are computed from the component endpoints. Components with "manufacturability margin" (Δt^k, defined as $t^k - t_{min}^k$) less than zero cannot be produced and should not be permitted by the optimizer. The build direction is specified manually.

This manufacturability information is integrated into the bcMMC method by penalizing the component density of unmanufacturable features. Because the optimization formulation already penalizes intermediate-density elements (using p in Eqn. (1b)), the optimizer is incentivized to either bring them back to full density (by thickening them or changing the angle/shape of the feature) or shrink them until they reach zero density, removing them from the solution. Density penalization based on member thickness is used successfully by Norato et al. [15], where non-integer components were penalized so that the design could be realized using readily-available stock material. A penalization approach has the additional benefit of allowing the optimizer to remove components from the problem by exploiting the penalization to assign them zero density, something difficult in other MMC implementations.

The bulk density of a component is controlled by specifying the maximum value of the smoothed Heaviside projection, i.e. by setting $\bar{\rho}$ in Eqn. (3). Reducing $\bar{\rho}$ from unity causes the entire interior of a component to become less dense (see Figure 4f). Ideally, the bulk density of the component should transition from solid to void as the manufacturability margin drops to zero. To avoid discontinuities, the transition is governed by another application of the smoothed Heaviside function, this time with (new) smoothing parameter γ. Equation (3) can be rewritten

$$\begin{aligned} \rho_e(\mathbf{z}) &= \max_{k=1..n_c} H\left(\phi\left(x_e, y_e, \mathbf{c}^k\right), \epsilon, \bar{\rho}^k\right) \\ \bar{\rho}^k &= H\left(\Delta t^k, \gamma, 1\right) \\ \Delta t^k &= t^k - t_{min}(\mathbf{c}^k) = t^k - S(l^k, \theta^k) \end{aligned} \tag{5}$$

Note that a formula for explicit derivatives could still be obtained, despite the added interaction between $\bar{\rho}^k$ and $\mathbf{z}$, because the constraint function S is differentiable. Numeric derivatives are used in this implementation, however.

The above approach handles manufacturability constraints for individual components. However, components often overlap to form larger effective structures in MMC solutions. Since longer features require larger minimum diameters to be manufacturable, two individually manufacturable features could

join end to end to create an unmanufacturable result. To overcome this difficulty, component endpoints are explicitly merged in the bcMMC approach, producing "chains" of components linked end-to-end to create a larger equivalent feature that can also be evaluated for manufacturability.

As a heuristic to prevent chains from forming unmanufacturable features, the components in the chain are combined into an "equivalent component" created by taking the average angle, average thickness, and total length of the chain elements (see Figure 6). A thickness margin for the equivalent chain is obtained by querying the constraint function using the equivalent component's shape parameters. The bulk density ($\bar{\rho}$) for all components in a chain is redefined to use the smallest of the thickness margins of each chain component and of the equivalent component. This causes entire chains to be removed all at once from the design space, preventing dangling components which are not supported from forming.

Experimental evidence suggests a continuation approach which slowly decreases the smoothing parameter γ over the first 40-80 iterations allows the optimizer time to thicken components before they are reduced to zero density. Such an approach is used here.

One additional minor implementation detail is of note: To avoid having the optimizer exploit the volume constraint by placing part of a component (partly) outside the analysis domain, the locations of the junction points are required to remain away from the domain boundary, except on edges with symmetry boundary conditions and on the build plate (geometry on the build plate is assumed to be more easily producible because it is everywhere supported). This "Endpoint Keep-out Zone" is specified in the problem definition and works to keep most of the component mass inside the domain, so that the FEA, volume constraint, and manufacturability assessment can all be applied uniformly (see Figure 7). It does not add any effectiveness to the bcMMC approach, only avoids unrealistic results.

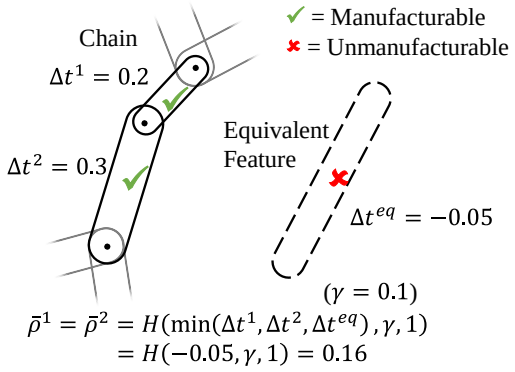

Figure 6. Example of Chained Components

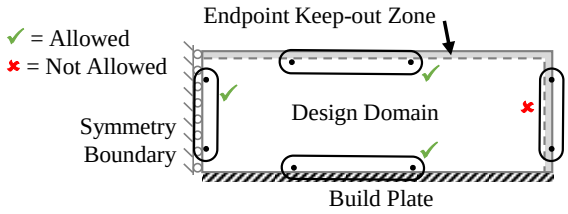

Figure 7. Endpoint Keep-out Zone (showing allowable feature placements)

RESULTS

In this section, some preliminary results obtained using the bcMMC approach are presented. First, a validation study evaluates the bootstrapping approach, followed by two examples demonstrating the value of using feature-driven manufacturability penalties. Unless otherwise stated, parameters for all problems in this section are shown in Table 1, where w_e and w_d correspond to the width of an element and of the domain, respectively. The optimizer used is the Method of Moving Asymptotes algorithm by Svanberg [27]; SIMP results are generated using the *top110* code by Andreassen et al. [28] utilizing the projection filter from [13].

Table 1. Default parameters

Parameter	**Value**
Fully dense elastic modulus E	1
Void elastic modulus E_{min}	10^{-9}
Poisson's ratio ν	0.3
Intermediate density penalty p	3
SIMP iterations before bootstrapping	50
Heaviside smoothing for edges ϵ	$0.5w_e$ [a]
Initial smoothing for bulk penalization γ_0	$0.1w_d$ [b]
Final smoothing for bulk penalization γ_f	$0.008w_d$ [b]
Steps used in the continuation of γ	60
MMC Derivative step size, x and y	$2w_e$ [a]
MMC Derivative step size, t	$0.2w_e$ [a]
l_{min} used in bootstrapping	0.1 mm (0.039 in)

[a] w_e refers to the width of an element (in domain units)
[b] w_d refers to the width of the domain (in domain units)

Convergence of bcMMC

Because SIMP quickly provides an initial configuration close to a local minimum, the bootstrapping approach is expected to converge more quickly to a good solution. To evaluate this assumption a compliance minimization in the 160x80 element domain (2:1 aspect ratio) shown in Figure 8a is considered. It is solved using three approaches: (1) Using only SIMP; (2) using only the main MMC framework with a set of isolated components in the initial condition shown in Figure 8b (as in [15]); and (3) using the bcMMC technique with 50 SIMP iterations. The volume fraction is set to 40%, and the minimum feature size is set to 2.4 element widths. For this trial, the keep-out zone is disabled and no manufacturability penalties are applied.

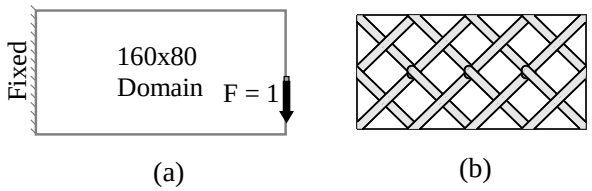

Figure 8. (a) Design Domain (b) Initial Component Distribution

Summary results are presented in Table 2. The iteration history plot (shown in Figure 9) shows that the SIMP result quickly converges to a low (good) objective function value, beyond which slow, steady improvement is seen.

Table 2. Bootstrapping Test Results

Solver	Conditions	Output Density Field	Output Component Plot
SIMP	Minimum feature size of 2.4 elements	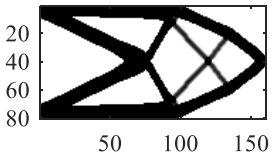 400 iterations, $\bar{f} = 74.88$	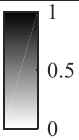
Non-bootstrapped MMC	No manufacturing penalty 16 unlinked components Minimum t of 2.4 elements No keep-out zone	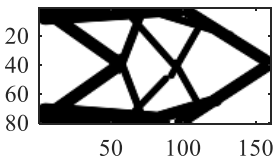 400 iterations, $\bar{f} = 78.97$	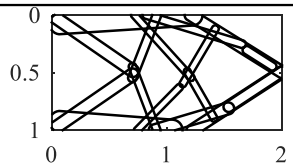
Bootstrapped bcMMC	No manufacturing penalty No keep-out-zone 50 Iteration SIMP bootstrap Minimum t of 2.4 elements $l_{min} = 2.4$ elements	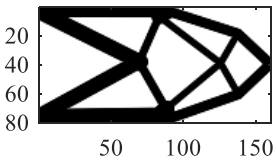 50 SIMP + 146 bcMMC iterations, $\bar{f} = 76.14$	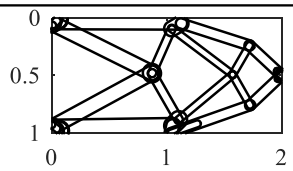

The non-bootstrapped MMC solution converges slowly due to the need to move each individual component into position, but ultimately reaches an objective function value 5.4% higher than SIMP. The bootstrapping process creates an initial component layout after 50 iterations of SIMP, after which a few iterations of higher objective are seen as the optimizer adjusts for irregularities introduced by the bootstrapping process, but then drops quickly to an objective function value only about 1.6% higher than SIMP, stopping after only 146 MMC iterations. The optimization is stopped when the largest iteration-to-iteration change in any entry in the state vector **z** drops below 0.1% of its allowable range.

To quantitatively assess the differences in convergence, the number of iterations required for thresholded compliance to drop and remain below 80 is considered (see dashed line in Figure 9). The bcMMC solution reaches this threshold in 70 iterations, which though worse than SIMP is a 72% improvement over non-bootstrapped MMC. SIMP consistently outperforms unconstrained bcMMC; however SIMP is unable to incorporate the feature-driven manufacturing constraints which are the focus of this work.

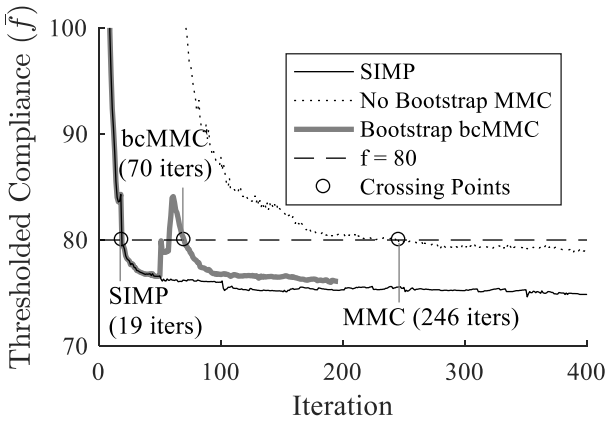

Figure 9. Bootstrapping Test Convergence (lower values are better)

The Short Beam Problem

The short beam problem considers the design of a manufacturable cantilevered beam with the configuration shown in Figure 10. The 200x100 FEA domain measures 40 mm by 20 mm (1.57 in by 0.79 in). The build plate and keep-out zone definition for this problem are also shown in Figure 10. The SIMP filter size is set to create 0.6mm (0.024 in) minimum features, a thickness which is just below the smallest value for any feature at any orientation or length in the manufacturing constraint function for the process used. The volume fraction is set to 50%. The SIMP algorithm is run for 50 iterations prior to bootstrapping, and the main optimization code allowed to run until convergence up to 200 additional iterations.

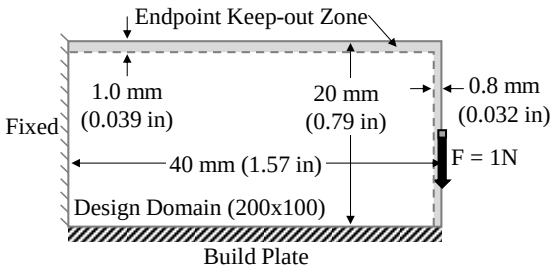

Figure 10. Setup for the short beam problem

Intermediate results for the bootstrapping are shown in Figure 11. After 50 iterations, the SIMP code produces geometry with fine details (Figure 11a), but some are lost in the conversion to component layout shown in Figure 11b. The small features which are removed have a relatively minor impact on the overall performance of the structure, and are likely not manufacturable anyway.

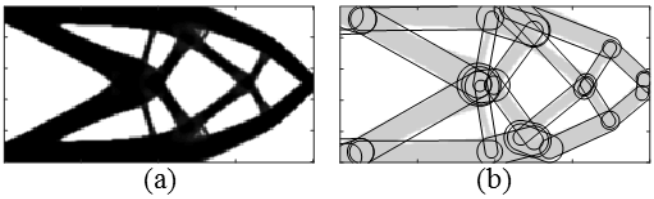

Figure 11. Bootstrapping for the Short Beam Problem (a) SIMP Result (b) Component Layout

Table 3 show the bcMMC layouts and density fields for two different build directions. In both cases, the manufacturability penalty is active. In the top row, the build direction is orthogonal to the build plate shown in Figure 10. All of the small features present in the SIMP design are retained, though some are reshaped, resulting in a thresholded compliance 1.2% higher than a reference SIMP solution with minimum feature size of 1.0 mm (0.039 in, large enough to generally be manufacturable on the selected process for overhang angles less than 45°). Note that in contrast to the reference SIMP solution, the results of both bcMMC solutions presented in Table 3 fully satisfy the parametric minimum feature size design rule and should be manufacturable. Even though many overhanging members exist in this configuration, they all lie above the experimentally-determined minimum feature diameter for their respective orientations.

Table 3. Short Beam Problem Results

Solver	Conditions	Output Component Plot	Output Density Field
bcMMC	Build direction 0° $V_f = 0.5$	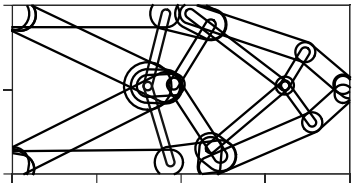	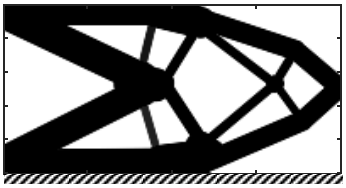
		50+200 iterations, $\bar{f} = 62.39$ (+1.2%)	
bcMMC	Build direction 90° $V_f = 0.5$	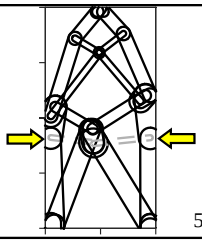	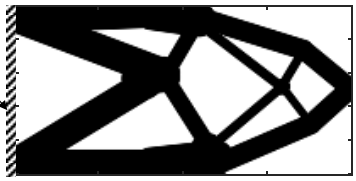
		50+200 iterations, $\bar{f} = 62.55$ (+1.5%)	

In the second row of Table 3, the same problem is solved, with the build direction rotated 90°. In this case, most components are more easily manufactured, except for two nearly-horizontal components (see arrows) which have been removed as inefficient by the optimizer by thinning until the effective density is zero and redistributing their material to other components. The objective function value for this case, $\bar{f} = 62.55$, lags the SIMP solution by 1.45%. The central large features in this design show some asymmetry due to sensitivity of the shape skeleton operation used in bootstrapping which resulted in uneven penalization of the two horizontal components, and is a clear shortcoming of this approach. Several intermediate steps from this case are shown in Figure 12.

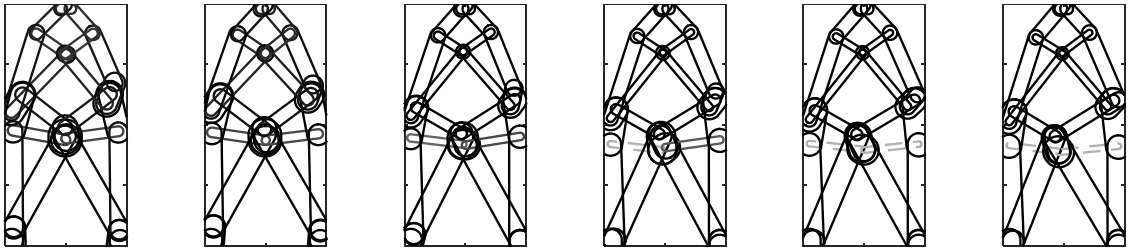

Figure 12. Intermediate results for the rotated Short Beam Problem.

The MBB Beam Problem

The well-known MBB problem [10] is also solved; Figure 13 shows half of the symmetric design domain modelled by 225x75 FEA elements and measuring 45mm by 15 mm (3:1). The SIMP implementation used for bootstrapping employs a p-continuation approach which yields the more intricate microstructure in the center of the domain by incrementing p from 1.0 to 3.0 in steps of 0.1 every 50 iterations. After p reaches

3.0, the beta parameter of the Heaviside projection filter of Guest et al. [13] is incremented until either convergence is reached or when 1200 iterations have occurred. The SIMP filter ensures at least 0.6mm (0.024 in) thick features, which is just less than the smallest manufacturable feature size. The volume fraction is set to 40%. Because of the continuation used, bootstrapping is performed after all 1200 SIMP iterations, producing the result shown in Figure 14.

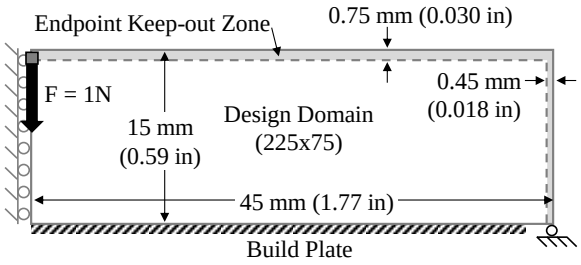

Figure 13. Setup for the MBB Problem

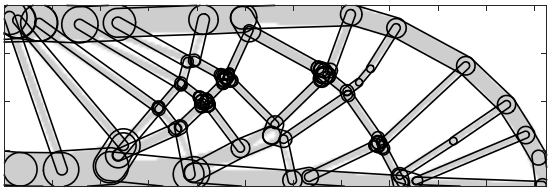

Figure 14. SIMP solution for Bootstrapping in the MBB Problem (with components overlaid)

Table 4. MBB Problem Results

Case	Design	Manufactured Structure
SIMP, 0.71 mm (0.028 in) minimum member thickness. 1200 iterations, $\bar{f} = 225.77$		
SIMP, 1.0 mm (0.039 in) minimum member thickness. 1200 iterations, $\bar{f} = 219.43$		
bcMMC, 1200+200 iterations, $\bar{f} = 222.35$		
Build Plate		10mm (0.394 in)

Table 4 shows three manufactured designs, 3D printed on a Flashforge Finder material extrusion printer using polylactic acid (PLA) filament with identical process settings. All three struggle with surface finish in the overhanging features however the drooping in the very thin members in the more aggressive SIMP case (with minimum member thickness of 0.71 mm or 0.028 in) results in a significant fraction of each

beam not being fully manifested. The bcMMC optimizer adjusts the overhang angle and thickness of major features in the design to be better supported and thickens some of the smaller elements to increase manufacturing performance (see arrows in Table 4). The ability of the manufacturing constraint to allow bridging members enables the top element to be retained without additional supports, unlike the other overhang topology optimization approaches surveyed.

CONCLUSION

A data-driven constraint function for topology optimization of designs for AM developed previously has been incorporated into a Moving Morphable Components (MMC) topology optimization framework. To support this constraint, which provides a different minimum member thickness based on the shape and orientation of each straight segment in a design, a variant of the MMC framework is presented which utilizes SIMP to generate preliminary designs to serve as starting points. This "bootstrapped constrained MMC" approach (bcMMC) implements this manufacturability constraint and provides faster convergence to optimized solutions than reference MMC implementations.

Compared to other manufacturing constraints on topology optimization for AM, which typically utilize a single fixed minimum feature size and a maximum overhang angle, this functional constraint method helps take better advantage of the space of manufacturable geometries, increasing the design complexity the optimizer can achieve. For example, short horizontal "bridging" features can be included, providing solutions which more nearly match the unconstrained case while still being manufacturable.

The compliance minimization examples presented use a constraint function created for a material extrusion AM platform, but the approach is appropriate for generalization to other objective functions and AM processes. The modified optimization process ensures the design is both optimized *and* manufacturable, and makes relatively small changes to the part topology, component orientation, and component size compared to fixed minimum feature size techniques, with a penalty to the objective function of less than 5%.

Exciting possible extensions of this work include adapting the approach to 3D problems, different objective functions, and other AM processes, but these extensions are nontrivial and would require further research. Automatically generating and incorporating additional components to act as support material for overhanging features would also be advantageous.

ACKNOWLEDGMENTS

This work was partially supported by the National Science Foundation Graduate Research Fellowship Program under Grant No. DGE-1256082. Any opinions, findings, and conclusions or recommendations

expressed in this material are those of the author(s) and do not necessarily reflect the views of the National Science Foundation. An early version of the paper was presented at ASME IDETC 2018 [29].

REFERENCES

[1] Liu, Jikai, and Ma, Yongsheng. “A Survey of Manufacturing Oriented Topology Optimization Methods” Advances in Engineering Software Vol. 100 (2016): pp. 161–175. DOI 10.1016/j.advengsoft.2016.07.017.

[2] Coelho, Pedro, Cardoso, João, Fernandes, Paulo, and Rodrigues, Hélder. “Parallel Computing Techniques Applied to the Simultaneous Design of Structure and Material” Advances in Engineering Software Vol. 42 No. 5 (2011): pp. 219–227. DOI 10.1016/j.advengsoft.2010.10.003.

[3] Gu, X.J., Zhu, Jihong, and Zhang, W.H. “The Lattice Structure Configuration Design for Stereolithography Investment Casting Pattern Using Topology Optimization” Rapid Prototyping Journal Vol. 18 No. 5 (2012): pp. 353–361. DOI 10.1108/13552541211250355.

[4] Vayre, Benjamin, Vignat, Frédéric, and Villeneuve, François. “Designing for Additive Manufacturing” Procedia CIRP Vol. 3 (2012): pp. 632–637. DOI 10.1016/j.procir.2012.07.108.

[5] Zhou, M., and Rozvany, G.I.N. “The COC Algorithm, Part II: Topological, Geometrical and Generalized Shape Optimization” Computer Methods in Applied Mechanics and Engineering Vol. 89 No. 1–3 (1991): pp. 309–336. DOI 10.1016/0045-7825(91)90046-9.

[6] Weiss, Benjamin, Diegel, Olaf, Storti, Duane, and Ganter, Mark. “A Process for Estimating Minimum Feature Size in Selective Laser Sintering” Rapid Prototyping Journal Vol. 24 No. 4 (2018).

[7] Weiss, Benjamin, Hamel, Joshua, Storti, Duane, and Ganter, Mark. “Towards a General Method for Constructing Manufacturability Design Rules for an Additive Manufacturing Process” Additive Manufacturing, submitted (2019).

[8] Weiss, Benjamin, 2017, “Development of a Process for Determining Minimum Feature Size in Additive Manufacturing with Applications to Topology Optimization” University of Washington, PhD Dissertation, URI http://hdl.handle.net/1773/40934.

[9] Guo, Xu, Zhang, Weisheng, and Zhong, Wenliang. “Doing Topology Optimization Explicitly and Geometrically—A New Moving Morphable Components Based Framework” Journal of Applied Mechanics Vol. 81 No. 8 (2014): p. 081009. DOI 10.1115/1.4027609.

[10] Bendsøe, Martin, and Sigmund, Ole. Topology Optimization: Theory, Methods, and Applications. Springer, Berlin, Germany (2003).

[11] Deaton, Joshua, and Grandhi, Ramana. “A Survey of Structural and Multidisciplinary Continuum Topology Optimization: Post 2000” Structural and Multidisciplinary Optimization Vol. 49 No. 1 (2014): pp. 1–38. DOI 10.1007/s00158-013-0956-z.

[12] Sigmund, Ole, and Maute, Kurt. “Topology Optimization Approaches: A Comparative Review” Structural and Multidisciplinary Optimization Vol. 48 No. 6 (2013): pp. 1031–1055. DOI 10.1007/s00158-013-0978-6.

[13] Guest, James, Prévost, Jean, and Belytschko, Ted. “Achieving Minimum Length Scale in Topology Optimization Using Nodal Design Variables and Projection Functions” International Journal for Numerical Methods in Engineering Vol. 61 No. 2 (2004): pp. 238–254. DOI 10.1002/nme.1064.

[14] Deng, JiaDong, and Chen, Wei. “Design for Structural Flexibility Using Connected Morphable Components Based Topology Optimization” Science China Technological Sciences Vol. 59 No. 6 (2016): pp. 839–851. DOI 10.1007/s11431-016-6027-0.

[15] Norato, Julian, Bell, B.K., and Tortorelli, Daniel. “A Geometry Projection Method for Continuum-Based Topology Optimization with Discrete Elements” Computer Methods in Applied Mechanics and Engineering Vol. 293 (2015): pp. 306–327. DOI 10.1016/j.cma.2015.05.005.

[16] Zhang, Weisheng, Yuan, Jie, Zhang, Jian, and Guo, Xu. “A New Topology Optimization Approach Based on Moving Morphable Components (MMC) and the Ersatz Material Model” Structural and Multidisciplinary Optimization Vol. 53 No. 6 (2016): pp. 1243–1260. DOI 10.1007/s00158-015-1372-3.

[17] Bremicker, Michael, Chirehdast, Mehran, Kikuchi, Noboru, and Papalambros, Panos. “Integrated Topology and Shape Optimization in Structural Design” Mechanics of Structures and Machines Vol. 19 No. 4 (1991): pp. 551–587. DOI 10.1080/08905459108905156.

[18] Siddiqi, Kaleem, and Pizer, Stephen, eds. Medial Representations: Mathematics, Algorithms and Applications. Springer, Dordrecht, Netherlands (2008).

[19] Chang, Kuang-Hua, and Tang, Poh-Soong. “Integration of Design and Manufacturing for Structural Shape Optimization” Advances in Engineering Software Vol. 32 No. 7 (2001): pp. 555–567. DOI 10.1016/S0965-9978(00)00103-4.

[20] Lazarov, Boyan, Wang, Fengwen, and Sigmund, Ole. “Length Scale and Manufacturability in Density-Based Topology Optimization” Archive of Applied Mechanics Vol. 86 No. 1–2 (2016): pp. 189–218. DOI 10.1007/s00419-015-1106-4.

[21] Osanov, Mikhail, and Guest, James. “Topology Optimization for Additive Manufacturing Considering Layer-Based Minimum Feature Sizes.” Proceedings of the ASME IDETC/CIE. DETC2017-68383: p. V02AT03A036. Cleveland, OH, August 6, 2017. DOI 10.1115/DETC2017-68383.

[22] Hoang, Van-Nam, and Jang, Gang-Won. “Topology Optimization Using Moving Morphable Bars for Versatile Thickness Control” Computer Methods in Applied Mechanics and Engineering Vol. 317 (2017): pp. 153–173. DOI 10.1016/j.cma.2016.12.004.

[23] Driessen, A. M. “Overhang Constraint in Topology Optimisation for Additive Manufacturing: A Density Gradient Based Approach.” PhD Thesis. Delft University of Technology, Delft, Netherlands. 2016.

[24] Gaynor, A.T. and Guest, J.K. “Topology optimization considering overhang constraints: Eliminating sacrificial support material in additive manufacturing through design” Struct Multidisc Optim Vol. 54 (2016): 1157.

[25] Guo, Xu, Zhou, Jianhua, Zhang, Weisheng, Du, Zongliang, Liu, Chang, and Liu, Ying. “Self-Supporting Structure Design in Additive Manufacturing through Explicit Topology Optimization” Computer Methods in Applied Mechanics and Engineering Vol. 323 (2017): pp. 27–63. DOI 10.1016/j.cma.2017.05.003.

[26] Langelaar, Matthijs. “An Additive Manufacturing Filter for Topology Optimization of Print-Ready Designs” Structural and Multidisciplinary Optimization Vol. 55 No. 3 (2017): pp. 871–883. DOI 10.1007/s00158-016-1522-2.

[27] Svanberg, Krister. “The Method of Moving Asymptotes—a New Method for Structural Optimization” International Journal for Numerical Methods in Engineering Vol. 24 No. 2 (1987): pp. 359–373. DOI 10.1002/nme.1620240207.

[28] Andreassen, Erik, Clausen, Anders, Schevenels, Mattias, Lazarov, Boyan, and Sigmund, Ole. “Efficient Topology Optimization in MATLAB Using 88 Lines of Code” Structural and Multidisciplinary Optimization Vol. 43 No. 1 (2011): pp. 1–16. DOI 10.1007/s00158-010-0594-7.

[29] Weiss, B., Hamel, J., Ganter, M., and Storti, D., 2018, “Data-Driven Additive Manufacturing Constraints for Topology Optimization” Proceedings of the ASME IDETC/CIE Conference, Quebec City, Quebec, August 2018, DETC2018-85391.